DOI: 10.13009/EUCASS2019-1050

A GNSS RTK Positioning Algorithm Utilizing MCAR and AEKF for Medium Baseline

Cao Jing and Xue Xiaoqin***
**Beijing Institute of Space Long March Vehicle,China*
979838093@qq.com
***Beijing Institute of Space Long March Vehicle,China*
2267746873@qq.com

Abstract
In order to improve the performance of GNSS RTK positioning, we propose a new RTK algorithm which combines MCAR with AEKF. In this algorithm, the MCAR method solves ionospheric delay, and the LAMBDA algorithm is used to improve the success probability of ambiguity fixing. The AEKF algorithm ensures the continuity and stability of RTK positioning. In the medium baseline experiment, the proposed algorithm is compared with traditional LAMBDA algorithm. The results show the proposed algorithm has the centimeter level positioning accuracy. Therefore, the proposed algorithm can be adapted to the complex scenes which need the high accuracy positioning.

1. Introduction

With the increasing popularity of Global Navigation Satellite Systems (GNSS) and the rapid operation of continuous operation reference stations (CORS) in major cities, short-baseline and medium baseline real-time kinematic(RTK) positioning will become a hot spot in the field of high-precision positioning. High-precision positioning using carrier phase will be widely used. Compared to the long-term precision single-point positioning, the short- and medium-baseline RTK has advantages in terms of first positioning time, positioning accuracy and dynamic performance.
The traditional carrier phase solution is to search for ambiguity by the least squares ambiguity decorrelation adjustment algorithm (LAMBDA), and the success rate and complexity of the calculation need to be improved. Multi-carrier ambiguity resolution (MCAR) can avoid the complex calculation of the traditional ambiguity search method. By combining the multi-frequency measurement values linearly, the combined measurement values with longer wavelengths are generated, which is beneficial to fix the ambiguity.

In literature[1], the single-frequency/multi-frequency LAMBDA algorithm for GPS/BDS dual-system RTK positioning is studied, and the advantages of dual-system in ambiguity resolution and positioning error are compared and analyzed. In literature[2], the GPS/BDS dual-system short-baseline RTK algorithm based on Kalman filter is studied. The ambiguity is solved by LAMBDA algorithm, and the implementation details are given. However, since the LAMBDA algorithm uses the double-difference pseudo-range observation to solve the float solution, the obtained ambiguity noise variance is large, which makes the ambiguity calculation result difficult to pass the acceptance test, and the success rate is not high. In literature[3-4], the performance analysis of the existing three-frequency ambiguity resolution method is carried out, and it is verified that the three-frequency ambiguity solution has different degrees of improvement in positioning accuracy. The literature [5-6] studied the multi-system combination positioning, combined with the measured data to verify the ambiguity resolution and positioning accuracy. The results show that the MCAR optimization algorithm is feasible.

In this paper, the combined RTK positioning is performed by using the two frequencies of L1/L2 of GPS and B1/B2/B3 of BDS. As the length of the baseline increases, the influence of the ionospheric delay and others on the ambiguity resolution increases gradually. Therefore, we propose the multi-frequency signal ambiguity resolution and adaptive extended Kalman filter (AEKF) RTK positioning solution. Then the implementation flow and positioning algorithm of RTK positioning are given. In the end, the data of two CORS stations are used to carry out the medium baseline experiment. The success rate and positioning error of the proposed algorithm are compared with the traditional GPS/BDS LAMBDA algorithm. The results show that the proposed method can better satisfy the user's reliability and the need of positioning accuracy.

DOI: 10.13009/EUCASS2019-1050

2. LAMBDA algorithm

The double-difference observation equation of pseudorange and carrier phase can be expressed as:

$$\begin{cases} \Delta P_i = AX + \varepsilon_{\Delta P} \\ \Delta \phi_i = AX - \lambda_i N_i + \varepsilon_{\Delta \phi} \end{cases} \tag{1}$$

where the A represents a linear coefficient matrix, ΔP_i and $\Delta \phi_i$ are the DD pseudorange and phase measurements, $X = (x, y, z)$ is baseline parameter, λ_i is wavelength, N_i is ambiguity, $\varepsilon_{\Delta P}$ and $\varepsilon_{\Delta \phi}$ are measurement noise corresponding to pseudorange and carrier phase.
The observation equation can be rewritten as:

$$L = B \begin{bmatrix} X \\ N \end{bmatrix} \tag{2}$$

Where B is the design matrix and L is the pseudorange and carrier phase observation. In order to estimate the above observation equations, the least squares criterion is applied. First, the float baseline parameters and the ambiguity vector are solved as :

$$\begin{bmatrix} \hat{X} \\ \hat{N} \end{bmatrix} = \left(B^T Q_L^{-1} B \right)^{-1} B^T Q_L^{-1} L \tag{3}$$

Where Q_L is the covariance matrix of the observation. Then the calculated covariance matrix of the baseline and ambiguity parameters can be expressed as:

$$Cov\left(\hat{X}, \hat{N} \right) = \left(B^T Q_L^{-1} B \right)^{-1} = \begin{pmatrix} Q_{\hat{X}} & Q_{\hat{X}\hat{N}} \\ Q_{\hat{N}\hat{X}} & Q_{\hat{N}} \end{pmatrix} \tag{4}$$

The integer least squares solution can be seen as the solution to the following minimization problem:

$$\min_N \left(\hat{N} - N \right) Q_{\hat{N}}^{-1} \left(\hat{N} - N \right), N \in Z^n \tag{5}$$

Finally, the de-correlation search can effectively obtain the integer ambiguity, so that the high-precision carrier phase observation without ambiguity can be obtained, and the precise positioning of the double-difference carrier phase can be realized.

3. Ambiguity resolution

3.1 Observation model of multi-frequency signals

The combined double-difference pseudo-code and the phase observation are linear combinations of the triple-frequency signals, which can be expressed as:

$$\Delta P_{(i,j,k)} = \frac{i \cdot f_1 \cdot \Delta P_1 + j \cdot f_2 \cdot \Delta P_2 + k \cdot f_3 \cdot \Delta P_3}{i \cdot f_1 + j \cdot f_2 + k \cdot f_3} \tag{6}$$

$$\Delta \phi_{(i,j,k)} = \frac{i \cdot f_1 \cdot \Delta \phi_1 + j \cdot f_2 \cdot \Delta \phi_2 + k \cdot f_3 \cdot \Delta \phi_3}{i \cdot f_1 + j \cdot f_2 + k \cdot f_3} \tag{7}$$

$$\Delta \phi_{(i,j,k)} = i \cdot \Delta \phi_1 + j \cdot \Delta \phi_2 + k \cdot \Delta \phi_3 \tag{8}$$

DOI: 10.13009/EUCASS2019-1050

Where i, j, k are any combination coefficients, f_i is the frequency of the signal, the carrier phase observation value of equation (7) is in meters, and the carrier phase observation value of equation (8) is in units of weeks.
The combined frequency, corresponding wavelength, and integer ambiguity are defined as:

$$f_{(i,j,k)} = i \cdot f_1 + j \cdot f_2 + k \cdot f_3 \tag{9}$$

$$\lambda_{(i,j,k)} = \frac{c}{i \cdot f_1 + j \cdot f_2 + k \cdot f_3} \tag{10}$$

$$\Delta N_{(i,j,k)} = i \cdot \Delta N_1 + j \cdot \Delta N_2 + k \cdot \Delta N_3 \tag{11}$$

3.2 MCAR algorithm

The ambiguity resolution of the multi-frequency signal is performed in the order of the ultra wide lane EWL, the wide lane WL and the narrow lane NL. The first step uses the geometrically independent TCAR algorithm to determine the EWL ambiguity of the BDS. The second step uses the least squares solution of the BDS EWL carrier phase observation with fixed ambiguity, and uses the LAMBDA algorithm to search for BDS WL and GPS WL ambiguity. The third step is to combine the BDS WL and GPS WL carrier phase observations with the ambiguity and the BDS NL and GPS NL carrier phase observation simultaneous equations to obtain the least squares solution and obtain the BDS NL and GPS NL ambiguity using the LAMBDA algorithm. Finally, the ambiguity of each frequency signal of BDS/GPS can be calculated according to the fixed BDS WL and GPS WL ambiguity and BDS NL and GPS NL ambiguity.

(1) EWL ambiguity resolution
A geometrically independent model is constructed for the triple-frequency signal of the BDS system. Using its carrier phase and pseudo-range observation, the EWL solution equation of the ultra-wide lane is as follows:

$$\Delta N_{(0,-1,1),B} = \left[\Delta\phi_{(0,-1,1),B} - \frac{\Delta\rho_{(0,1,1),B}}{\lambda_{(0,-1,1),B}} \right]_{round} \tag{12}$$

Among them, the subscript ‘B’ indicates the BDS system, the EWL carrier phase combination is $(0,-1,1)$, and the combined pseudorange is $(0,1,1)$. Through various experimental analysis before, it can be determined that the EWL ambiguity solving by the formula (12) is simple and reliable.

(2) WL ambiguity resolution
After successfully determining the EWL ambiguity, the geometric model of the BDS/GPS combination is constructed to enhance the ambiguity solving model. For BDS satellites and GPS satellites, although their satellite positions are different, and the double-difference geometric distance from the receiver is different, but since the two receivers are fixed in position, the baseline vectors b_{ur} of the BDS system and the GPS system are common parameters. Therefore, we can construct a two-system observation equation in equation (13):

$$\begin{bmatrix} \Delta\hat{\rho}_{(0,-1,1),B} \\ \Delta\phi_{(1,0,-1),B} \cdot \lambda_{(1,0,-1),B} \\ \Delta\phi_{(1,-1,0),\mathrm{G}} \cdot \lambda_{(1,-1,0),\mathrm{G}} \end{bmatrix} = \begin{bmatrix} A_B & 0 & 0 \\ A_B & I \cdot \lambda_{(1,0,-1),B} & 0 \\ A_G & 0 & I \cdot \lambda_{(1,-1,0),\mathrm{G}} \end{bmatrix} \cdot \begin{bmatrix} b_{ur} \\ \Delta\hat{N}_{(1,0,-1),B} \\ \Delta\hat{N}_{(1,-1,0),\mathrm{G}} \end{bmatrix} + \begin{bmatrix} \varepsilon_{\Delta\hat{\rho}_{(0,-1,1),B}} \\ \varepsilon_{\Delta\phi_{(1,0,-1),B}} \\ \varepsilon_{\Delta\phi_{(1,-1,0),G}} \end{bmatrix} \tag{13}$$

Among them, the subscript ‘B’ indicates the BDS system, ‘G’ indicates the GPS system, $\Delta\hat{\rho}_{(0,-1,1),B}$ is the EWL distance without ambiguity, $\Delta\phi_{(1,-1,0),\mathrm{G}}$ indicates the WL ambiguity of the L1 and L2 signals combined by GPS, and

DOI: 10.13009/EUCASS2019-1050

$\lambda_{(1,0,-1),B}$ is the WL combined wavelength of BDS. $\lambda_{(1,-1,0),\mathrm{G}}$ is the WL combination wavelength of GPS. The geometric matrix A_B and A_G are designed by the cosine of the direction of observation.

For the float ambiguity $\Delta\hat{N}_{(1,0,-1),B}$ and $\Delta\hat{N}_{(1,-1,0),\mathrm{G}}$, the LAMBDA algorithm is used to search for the integer ambiguity, and the ambiguity of the BDS WL combination can be derived from the linear relationship.

(3) NL ambiguity resolution

In the solution of the first two steps, we obtained the super wide lane and wide lane ambiguity of BDS, and the wide lane ambiguity of GPS. Here, we consider the ionospheric delay of the BDS satellite and the GPS satellite separately. Using the original carrier phase observation of the B1 signal and the original carrier phase observation of the L1 signal, the calculation equation of equation (14) can be obtained:

$$\begin{bmatrix} \Delta\hat{\rho}_{(1,0,-1),B} \\ \Delta\hat{\rho}_{(1,-1,0),B} \\ \Delta\phi_{(1,0,0),B}\cdot\lambda_{(1,0,0),B} \\ \Delta\hat{\rho}_{(1,-1,0),\mathrm{G}} \\ \Delta\phi_{(1,0,0),\mathrm{G}}\cdot\lambda_{(1,0,0),\mathrm{G}} \end{bmatrix} = \begin{bmatrix} A_B & 0 & 0 & c1\cdot I & 0 \\ A_B & 0 & 0 & c2\cdot I & 0 \\ A_B & I\cdot\lambda_{(1,0,0),B} & 0 & I & 0 \\ A_G & 0 & 0 & 0 & g\cdot I \\ A_G & 0 & I\cdot\lambda_{(1,0,0),\mathrm{G}} & 0 & I \end{bmatrix} \cdot \begin{bmatrix} b_{ur} \\ \Delta\hat{N}_{(1,0,0),B} \\ \Delta\hat{N}_{(1,0,0),\mathrm{G}} \\ \Delta I_{1,B} \\ \Delta I_{1,G} \end{bmatrix} + \begin{bmatrix} \varepsilon_{\Delta\hat{\rho}_{(1,0,-1),\mathrm{B}}} \\ \varepsilon_{\Delta\hat{\rho}_{(1,-1,0),\mathrm{B}}} \\ \varepsilon_{\Delta\phi_{(1,0,0),\mathrm{B}}} \\ \varepsilon_{\Delta\hat{\rho}_{(1,-1,0),\mathrm{G}}} \\ \varepsilon_{\Delta\phi_{(1,0,0),\mathrm{G}}} \end{bmatrix} \quad \textbf{(14)}$$

Among them, $\Delta\hat{\rho}_{(1,0,-1),B}$ and $\Delta\hat{\rho}_{(1,-1,0),B}$ are BDS combined observations without ambiguity , $\Delta\phi_{(1,0,0),\mathrm{B}}$ is B1 signal carrier phase observation of BDS, $\Delta\hat{\rho}_{(1,-1,0),\mathrm{G}}$ is GPS WL combination observation without ambiguity, and $\Delta\phi_{(1,0,0),\mathrm{G}}$ is GPS L1 signal carrier phase observation .

The unknown vectors in the observation equation are the baseline vector b_{ur}, the NL ambiguity $\Delta\hat{N}_{(1,0,0),B}$ of BDS, the NL ambiguity $\Delta\hat{N}_{(1,0,0),\mathrm{G}}$ of GPS, the first-order ionospheric delay $\Delta I_{1,B}$ of B1 signal of BDS, and the first-order ionospheric delay $\Delta I_{1,\mathrm{G}}$ of L1 signal of GPS. According to the ionospheric relationship between carrier signals of different frequencies, the coefficient can be derived as follows:

$$\begin{cases} c1 = \lambda^2_{(1,0,-1),B} / \lambda^2_{(1,0,0),B} \\ c2 = \lambda^2_{(1,-1,0,),B} / \lambda^2_{(1,0,0),B} \\ g = \lambda^2_{(1,-1,0),\mathrm{G}} / \lambda^2_{(1,0,0),\mathrm{G}} \end{cases} \quad \textbf{(15)}$$

4. AEKF RTK algorithm

The flow of the BSK/GPS dual system AEKF RTK positioning algorithm proposed in this paper is shown in Figure 1.

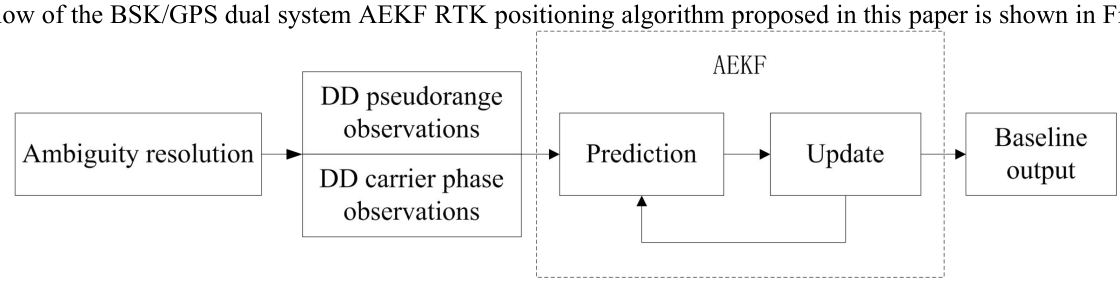

Figure 1: Flow chart of BDS/GPS AEKF RTK algorithm

The system state vector is as shown in equation (16) and contains the coordinates of the mobile station and the double difference ambiguity of the GPS L1/L2 and BDSB1/B2/B3 frequencies. The measurement vector is as shown in equation (17) and contains a double-difference carrier phase observation of 5 frequencies.

DOI: 10.13009/EUCASS2019-1050

$$X = \left[x, y, z, \Delta N_{B1}, \Delta N_{B2}, \Delta N_{B3}, \Delta N_{L1}, \Delta N_{L1}\right]^T \tag{16}$$

$$Z = \left[\Delta\phi_{B1}, \Delta\phi_{B2}, \Delta\phi_{B3}, \Delta\phi_{L1}, \Delta\phi_{L1}\right]^T \tag{17}$$

The prediction process of EKF is

$$\begin{cases} X_{k+1}^- = FX_k^+ \\ P_{k+1}^- = FP_k^+F^T + Q_w \end{cases} \tag{18}$$

In the formula, the subscript “k” represents the epoch time; the superscript “-” represents the a priori estimate, “+” represents the a posteriori estimate; F is the prediction matrix, and the static motion model is the unit matrix; P is the variance-variance of the state error; Q_w is the VC array of process noise, and it will be the zero matrix in the static motion model.
The measurement update process of EKF is

$$\begin{cases} K_{k+1} = P_{k+1}^- H^T \left(HP_{k+1}^- H^T + R_v\right)^{-1} \\ X_{k+1}^+ = X_{k+1}^- + K_{k+1}\left(Z_{k+1} - h\left(X_{k+1}^-\right)\right) \\ P_{k+1}^+ = \left(I - K_{k+1}H\right)P_{k+1}^- \end{cases} \tag{19}$$

Where K is the Kalman gain; $h\left(X_{k+1}^-\right)$ is the nonlinear functional relationship between the double-difference carrier phase observation and the system state vector; H is the measurement matrix, and $h\left(X_{k+1}^-\right)$ is the partial derivative of the system state, as shown in equation (20). R_v is a VC matrix for measuring noise, which is time-varying as the quality of the measurement changes, and is difficult to estimate by the model. Therefore, the adaptive method based on the innovation sequence shown in equation (21) is used for estimation.

$$H = \begin{bmatrix} A_B & \lambda_{B1}I & & & & \\ A_B & & \lambda_{B2}I & & & \\ A_B & & & \lambda_{B3}I & & \\ A_G & & & & \lambda_{G1}I & \\ A_G & & & & & \lambda_{G1}I \end{bmatrix} \tag{20}$$

$$R_v = \frac{1}{N}\sum_{j=k-N+1}^{k} v_j v_j^T - HP_k^- H^T \tag{21}$$

Among them, v is a new interest sequence, and $v_k = Z_{k+1} - h\left(X_{k+1}^-\right)$, N is an adaptive update period.

5. Experiment and analysis

In this paper, the medium baseline data with a length of 26.3km is selected for the experiments. The cutoff elevation angle of the satellite is 10°. The reference satellite selects the satellite with the highest elevation angle, and the broadcast ephemeris is used as the navigation file.

DOI: 10.13009/EUCASS2019-1050

5.1 LAMBDA algorithm experiments

Under the baseline condition, Figure 2 shows the positioning error of BDS/GPS. It can be seen that the error points at each moment are relatively unstable. Table 1 counts the root mean square value of the error.

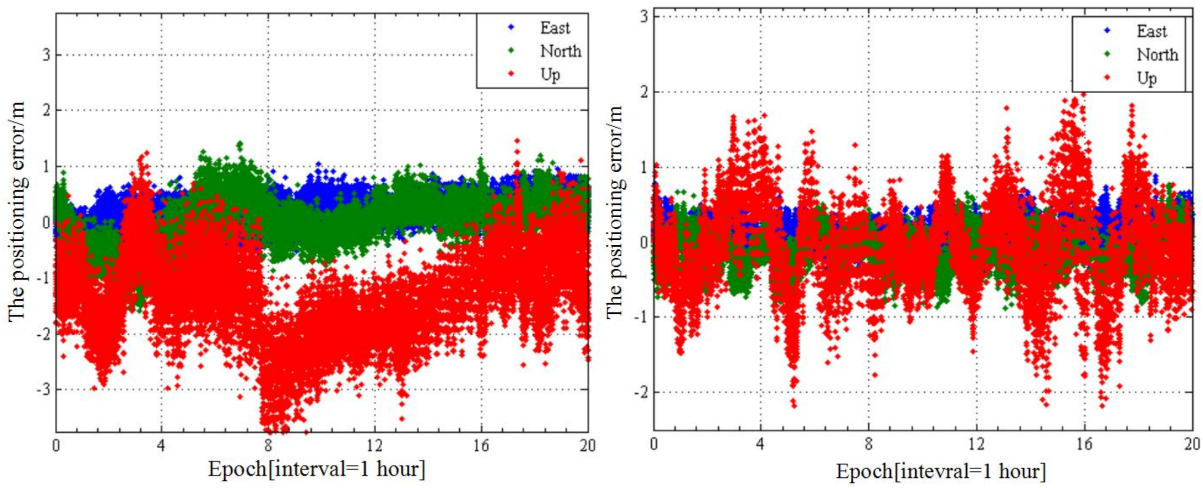

(a)BDS (b)GPS

Figure 2: The position accuracy of LAMBDA

Table 1: The RMS of position accuracy /m

	East	North	Up
BDS	0. 79	0.83	2.01
GPS	0. 69	0.76	1. 44

From the statistical results of Table 1, it is seen that under the medium baseline condition of 26.3 km, the positioning error of the BDS and GPS systems in the east (E) and north (N) directions is decimeter. And the positioning error in the up(U) direction is about two meters. So the ambiguity success rate obtained by directly using the LAMBDA algorithm is not high, and the more high-precision positioning result cannot be brought from this algorithm.

5.2 MCAR and AEKF RTK experiments

Under the medium baseline, the ionospheric delay of the B1 signal of the BDS system and the ionospheric delay of the GPS system L1 signal are shown in Figure 3. In this experiment, the visible satellites of BDS are C01, C02, C03, C04, C05, C06, C07, C08, C09, C10, C11, C12, which are respectively represented by different colors. GPS visible satellites are G02, G03, G09, G12 G13, G17, G19, G20, G23, G26, G28, G29 are respectively represented by different colors. When the current satellite is not received at the observation time, the ionospheric delay of the corresponding satellite in Figure 3 is represented by 0.

DOI: 10.13009/EUCASS2019-1050

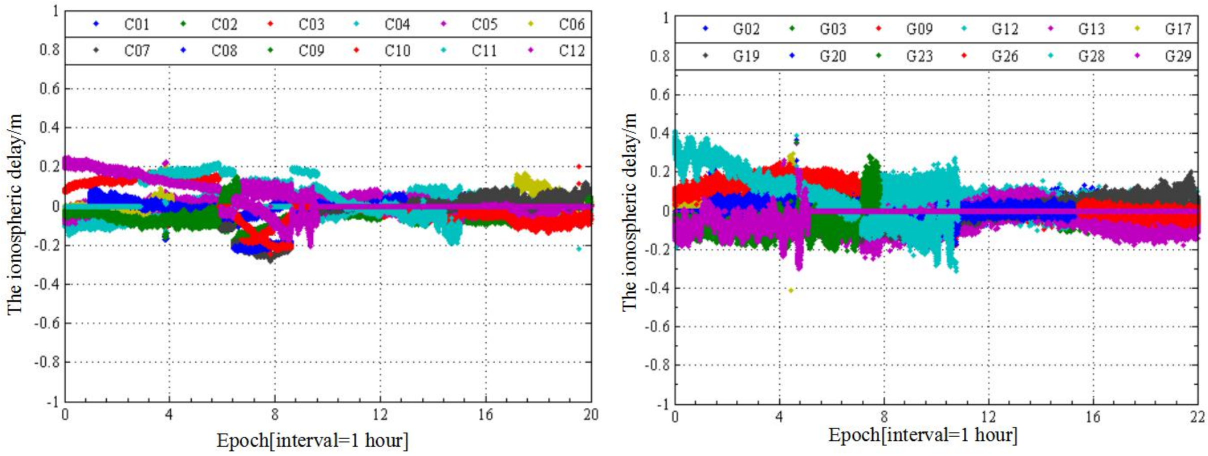

(a)BDS (b)GPS

Figure 3: The ionospheric delay

Table 2: The RMS of ionospheric delay (BDS system)/m

Satellite No	B01	B02	B03	B04	B05	B06
RMS	0.078	0.056	0.089	0.101	0.103	0.088
Satellite No	B07	B08	B9	B10	B11	B12
RMS	0.102	0.069	0.076	0.081	0.094	0.091

Table 3: The RMS of ionospheric delay (GPS system)/m

Satellite No	G02	G03	G09	G12	G13	G17
RMS	0.088	0.062	0.091	0.103	0.092	0.064
Satellite No	G19	G20	G23	G26	G28	G29
RMS	0.091	0.066	0.080	0.073	0.103	0.084

Table 2 counts the RMS value of some BDS satellite ionospheric delays. Table 3 shows the ionospheric delays of some GPS satellites. The results show that the ionospheric delays of BDS satellites and GPS satellites are all in the centimeter level, and the RMS values are basically less than 1 decimeter.

Under the medium baseline, the positioning error of combined BDS and GPS system for RTK solution is shown in Figure 4:

DOI: 10.13009/EUCASS2019-1050

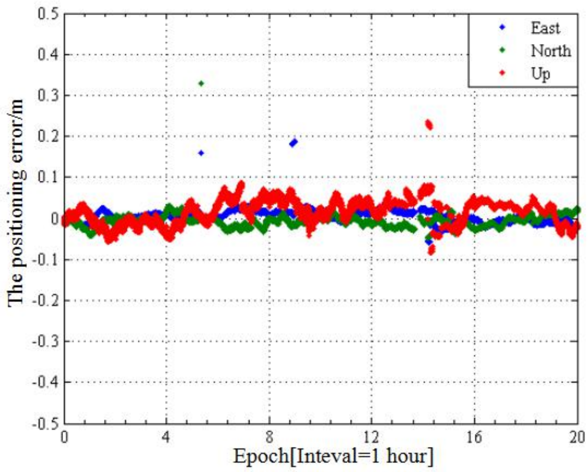

Figure 4: The position accuracy of MCAR and AEKF RTK

The RMS values of the positioning error in east direction is $RMS_E = 0.015$ m, the north direction is $RMS_N = 0.019$ m, and the up direction is $RMS_U = 0.035$ m. Respectively, the MCAR and AEKF RTK algorithm reduces the discrete error points of the distribution, and the centimeter-level positioning under the medium baseline can be achieved.

6. Conclusion

This paper proposes a combined MCAR and AEKF RTK positioning scheme. For the combined BDS and GPS system, the spatial geometric distribution characteristics of the satellite can be improved, the number of visible satellites participating in the positioning is increased, and it guarantees the continuity of positioning points. The MCAR algorithm can calculate the ionospheric delay and finally achieve a stable positioning of 5 cm under the medium baseline of 26.3 km. It shows that the scheme can be adapted to high-precision positioning scenarios in complex environments such as cities.

References

[1] He H , Li J , Yang Y , et al. Performance assessment of single- and dual-frequency BeiDou/GPS single-epoch kinematic positioning[J]. GPS Solutions, 2014, 18(3):393-403.
[2] Zhao S , Cui X , Guan F , et al. A Kalman Filter-Based Short Baseline RTK Algorithm for Single-Frequency Combination of GPS and BDS[J]. Sensors, 2014, 14(8):15415-15433.
[3] Tang W , Deng C , Shi C , et al. Triple-frequency carrier ambiguity resolution for Beidou navigation satellite system[J]. GPS Solutions, 2014, 18(3):335-344.
[4] Xiaohong Zhang, Xiyang He, Performance analysis of triple-frequency ambiguity resolution with BeiDou observations[J]. GPS Solut, 20:269–281, 2016.
[5] Jinming H . A Method of BDS/GPS RTK Positioning Based on MCAR Algorithm for Medium-baseline[J]. Geomatics & Information Science of Wuhan University, 2017, 42(9):1216-1222.
[6] Hou P, Zhang B, Yuan Y. Combined GPS+BDS instantaneous single-and dual-frequency RTK positioning: stochastic modelling and performance assessment[J]. Spatial Science, 2019(1):1-24.